The Construction and Use of Potential–pH Diagrams in Organic Oxidation–Reduction Reactions

Stuart I. Bailey and Ian M. Ritchie *
Department of Physical and Inorganic Chemistry, University of Western Australia, Nedlands, Western Australia 6009, Australia
Frank R. Hewgill
Department of Organic Chemistry, University of Western Australia, Nedlands, Western Australia 6009, Australia

Potential–pH diagrams were constructed from literature data for phenol, 2,4,6-tri-t-butylphenol, and hydroquinone (1,4-dihydroxybenzene). The relationship between chemical and electrochemical phenomena is described, and the significance of the results of chemical experiments discussed in relation to the potential–pH diagrams for the case of phenol oxidations.

Potential (E)–pH diagrams, sometimes called Pourbaix diagrams, are convenient ways of summarizing equilibrium information about reactions, particularly oxidation–reduction reactions, which take place in solution. The construction of an E–pH diagram has been described by Pourbaix.[1] Once constructed, it defines the range of potential and pH over which any species of interest is thermodynamically stable. E–pH diagrams can thus be used to predict whether or not two chemical species will react but of course, give no information whatsoever about the rate of reaction. If each of the two species occupy the same area on an E–pH diagram, they will coexist. On the other hand, if they occupy different areas on the E–pH diagram, they are likely to react. Using this principle, Pourbaix[1] has determined the conditions under which all common metals are likely to corrode in water.

It is worth pointing out that the electrochemical potential E is directly related to the free energy ΔG of the system by $\Delta G = -nFE$ where n is the number of electrons involved in the redox reaction and F is the Faraday constant. It follows, then, that an E–pH diagram can be simply transformed into a plot of the free energy of the system as a function of pH. It is not, however, just a matter of scaling, since allowance must be made for the number of electrons n involved in the various electrode reactions.

Considering the convenience of Pourbaix diagrams, it is surprising that relatively little use has been made of them in the field of organic chemistry. One of the few examples in the literature is that due to Waters[2] who used a simple two line E–pH diagram to determine the range of pH within which the oxidation of phenol would proceed *via* a one-electron step as opposed to a two-electron step. Although Waters' paper has been described as important,[3,4] little use has been made of E–pH diagrams and few have been published, although in some cases the basic data for their construction exists in the literature. The construction of an atlas of E–pH diagrams comparable with that devised by Pourbaix for the metals would seem desirable.

In this paper, we will briefly describe how a potential–pH diagram is constructed, and discuss the sort of approximations that are commonly made during its construction. A simple three-line diagram for phenol will be presented, and the generalization of this diagram to other substituted phenols described. The influence of the solvent on these diagrams will be briefly examined. Finally, we will describe the construction of two more complex E–pH diagrams for the compounds 2,4,6-tri-t-butylphenol in aqueous ethanol (57% w/w) as solvent and 1,4-dihydroxybenzene in water as solvent. Examples of the use of Pourbaix diagrams in discussing reaction mechanisms will be presented.

The Construction of Potential-pH *Diagrams.*—Potential–pH diagrams are a graphical representation of solution equilibria. Since all solution equilibria are dependent upon the temperature and pressure, these variables must be specified, the usual choice being 25 °C and 1 atm. It is also usual to specify a concentration for all solution species depicted on the diagram. However, the need to specify the concentration in the sorts of diagram we are considering here can be avoided by assuming that activity effects can be neglected, and that activities can be replaced by concentrations in all equilibrium expressions. It is then only necessary to stipulate that the concentration of all species must be equal along equilibrium lines.

Three types of line corresponding to three types of equilibria may be distinguished on an E–pH diagram.

(i) Acid–base equilibria are independent of potential and are represented by a vertical line on the E–pH diagram. The position of the line is fixed by the condition that the pH is equal to the pK_a.

(ii) Simple redox equilibria, in which electrons but not protons are transferred to interconvert oxidized and reduced forms, are represented on an E–pH diagram by a horizontal line. The position of the line is determined by the standard redox potential of the reaction.

(iii) Redox equilibria involving both protons and electrons may be written according to equation (1) where Ox and Red

$$a\text{Ox} + ne + h\text{H}^+ \rightleftharpoons r\text{Red} + w\text{H}_2\text{O} \qquad (1)$$

represent the oxidized and reduced forms respectively. Assuming equal concentrations of oxidized and reduced species, the Nernst equation for this reaction at 25 °C reduces to (2), *i.e.* the slope of the equilibrium line on an E–pH diagram is $-0.0592(h/n)$ V per pH unit.

$$E = E^{\ominus} - 0.0592(h/n)\text{pH} \qquad (2)$$

Methods of Determining E.—From the above, it can be seen that in order to construct the equilibrium line for any redox reaction, it is necessary to know the value of the equilibrium potential at some pH. In aqueous solution, this is usually quoted with respect to the standard hydrogen electrode. Although this information is normally available, it is notoriously difficult to obtain for most phenol redox systems since it is difficult to establish equilibrium mixtures of oxidized and reduced forms in solution. This is because aryloxyl radicals, formed by a one-electron oxidation, are usually destroyed by irreversible coupling, and aryloxenium ions, formed by a two-electron oxidation, may participate in
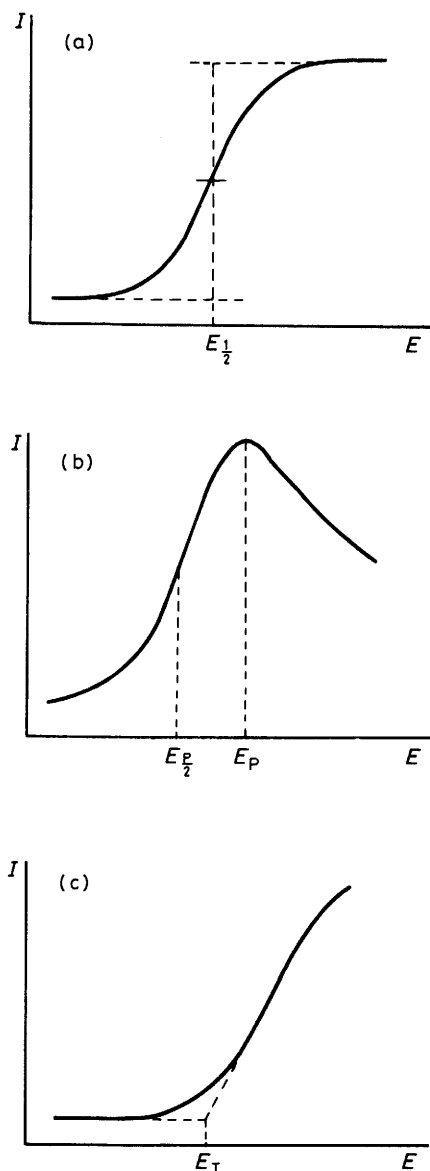
Figure 1. Schematic current-voltage diagrams (voltammograms) showing the measurement of characteristic potentials which may be related to the equilibrium potential: (a) half-wave potential $E_{\frac{1}{2}}$ from polarographic wave; (b) peak potential E_p and half peak potential $E_{p/2}$ from cyclic voltammetry; (c) tangent potential E_T from various voltammetric methods

Figure 2. Potential–pH diagram for phenol in aqueous solution. The points are included for comparison with the data from ref. 11, which is plotted as a bold line: ●, ref. 12; ■, ref. 10; ▲, ref. 13. Fine line is O_2 (1 atm.)–H_2O equilibrium

electrophilic aromatic substitution or undergo nucleophilic attack.

In the few cases where aryloxyl radicals are stable, it is possible to determine an equilibrium potential by potentiometric methods. Thus the equilibrium potentials for various 2,4,6-triarylphenols have been obtained by potentiometric titration.[5] When the oxidation products of a phenol are stable, the half-wave potential $(E_{\frac{1}{2}})$, which is a good approximation to the equilibrium potential,[6] can be obtained by polarography or cyclic voltammetry. However, when the oxidation products of a phenol are unstable, the voltammetric wave is no longer reversible, and it is difficult to determine the equilibrium potential from it. The difficulty lies in separating the unknown equilibrium potential from the unknown electrochemical rate constant. An additional, and common practical problem which occurs during the electrochemical oxidation of
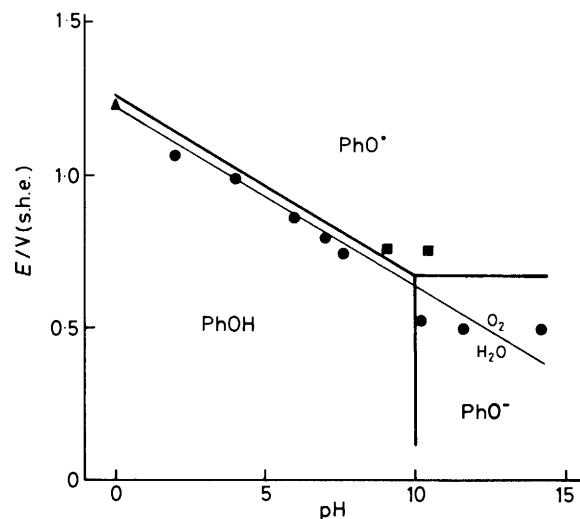
a phenol, is the formation of a non-conducting polymeric film on the electrode surface.[7,8]

Despite this uncertainty, it is common practice to use various quantities measured from the voltammetric wave as approximations to the equilibrium potential. Some of these are shown in Figure 1. They include the half wave potential $(E_{\frac{1}{2}})$ measured at a moving electrode such as the rotating disc, the peak potential (E_p) or half peak potential $(E_{p/2})$ measured at a stationary electrode, and the tangent potential (E_T). However, it must be stressed that none of these quantities can be simply related to the equilibrium potential for anything other than a reversible electrode reaction.

The E–pH Diagram for Phenol in Aqueous Solution.—It is known that phenol dissociates with a pK_a of 10.0,[9] and so the PhOH–PhO⁻ equilibrium is represented by a vertical line at pH 10.0. In order to fix the PhO·–PhOH line which has a slope of -0.0592 V per pH unit, and the PhO·–PhO line, which is horizontal, an equilibrium potential at some pH must be known. The results of Hedenberg and Frieser[10] are often quoted in this context since they do provide evidence that the half-wave potentials they measured were for the reversible one-electron oxidation of phenol. However, the design of their experiment was such that the evidence must be regarded with some reservation. For example, the measurements were made at a stationary electrode in a two electrode cell. Accordingly, we have preferred the results of Bub et al.,[11] who measured tangent potentials. For a reversible reaction $E_{\frac{1}{2}}$ and E_T differ by 0.066 V,[11] and so a better approximation to the equilibrium potential can always be obtained by adding 0.066 V to E_T, even when the reaction is irreversible, as in the oxidation of phenol. The results of Bub et al.[11] have been adjusted in this way, and are plotted in Figure 2 as a function of pH. The results of Vodzinskii et al. $(E_{\frac{1}{2}})$,[12] Hedenberg and Frieser $(E_{\frac{1}{2}})$,[10] and Penketh $(E_T + 0.066$ V),[13] have been included in Figure 2 for comparison. These results are essentially in agreement.

The O_2–H_2O equilibrium line has also been drawn on Figure 2, and lies below the PhO·–PhOH line. By analogy with Pourbaix' consideration of metal corrosion by water, this indicates that the phenoxyl radical could oxidize water. As always with this type of interpretation, there is no indication

that this reaction would proceed at an appreciable rate, especially in comparison with coupling.

Since the existence of the phenoxyl radical is so transient that no reverse electrochemical reaction is observed, it is not surprising that the electrochemical oxidation of the phenoxyl radical to the phenoxenium ion is also not observed. Were it observed, the equilibrium potential of such a reaction would, of course, be pH independent, as noted by Waters.[2] However, there is in the literature, a large amount of indirect evidence that the phenoxenium ion is formed, presumably by the two-electron oxidation of phenol or the phenoxide ion.[8,14-16] The bulk of this evidence is based on product analyses which show that nucleophilic substitution of the phenoxenium ion has occurred, but no suitable quantitative data seem to be available for inclusion in Figure 2. In certain substituted phenols such as 2,4,6-tri-t-butylphenol, the aryloxyl radical is sufficiently stable for the second electron transfer to be observed electrochemically. Systems of this type will be considered in a later section. We will first discuss substituted phenols whose behaviour is essentially similar to that of the parent compound.

Extension of the Diagram to Different Phenols.—It is well known that the acid dissociation constant pK_a for a variety of substituted phenols in the same solvent, for example, water, is linearly related to the Hammett substituent constant σ.[17] It has also been shown that the various approximations to the equilibrium potential ($E_{\frac{1}{2}}$, E_T, etc.) are linearly related to σ,[12,18,19] or equivalently, that the oxidation potential is linearly related to pK_a.[18] It follows that a three-dimensional Pourbaix diagram can be drawn with the Hammett σ parameter as the third axis. This plot, which would consist of plane surfaces, would encompass the behaviour of all substituted phenols which are relatively uncomplicated and whose properties can be correlated by means of the Hammett function. The three-dimensional plot can be simply portrayed by projecting the diagrams for representative values of σ onto the E-pH plane as shown in Figure 3. The correlation data, used to construct Figure 3 are taken from Rochester [17] and Ross *et al.*[18]

Extension of Diagram to Different Solvents.—We have so far only considered the construction of potential-pH diagrams for phenols in water. Such diagrams can, of course, be constructed for other solvents and solvent mixtures. It is known that the pK_a of an organic acid such as phenol increases as the acceptor number (Lewis acidity) of the solvent is increased.[20] It is also known that the equilibrium potential of the quinone-semiquinone radical ion redox couple shifts to more positive values as the acceptor number is increased.[21] If a similar systematic change in equilibrium potential (or one of its approximations) were observed for the phenoxyl radical-phenol redox couple, it should be possible to correlate the E-pH diagrams for a given phenol with acceptor number, and so construct a three-dimensional diagram with acceptor number as third axis depicting the domains of stability of the various phenolic species in any solvent system. Projections onto the E-pH plane of such a hypothetical diagram for different acceptor numbers are shown in Figure 4.

To the best of our knowledge, there is insufficient data available in the literature at the present time for such a diagram to be constructed. One problem which must be solved before Pourbaix diagrams in different solvents can be compared is that of the reference electrode against which potential measurements would be made. It is impossible to compare potentials measured against different reference electrodes in different solvents since the potential difference between reference electrodes in different solvents is not a fixed
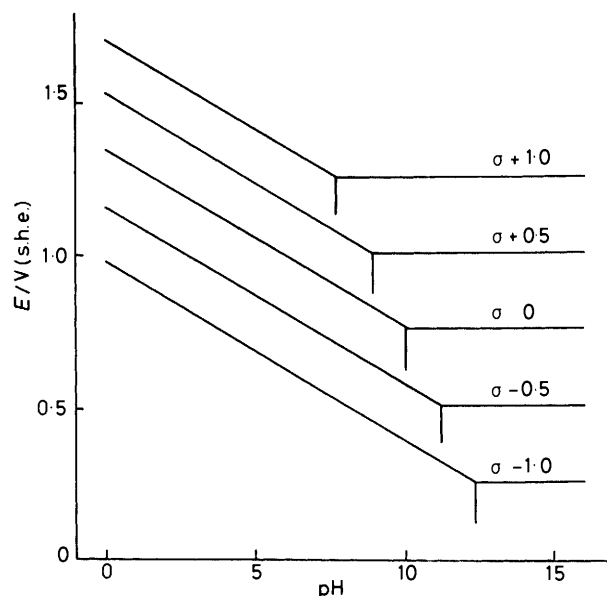

Figure 3. Projection of three-dimensional E-pH-σ diagram onto the E-pH plane for representative values of σ
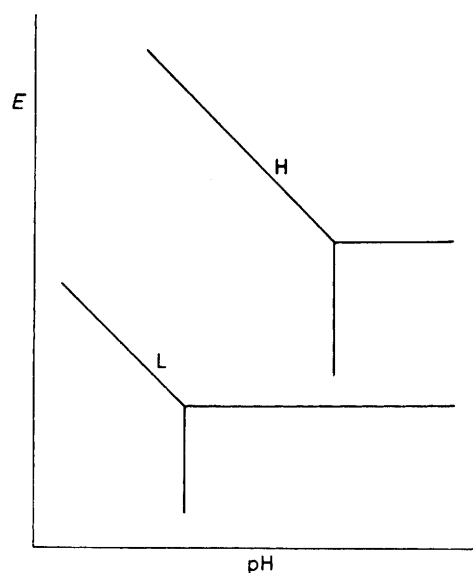

Figure 4. Schematic diagram of projection of phenol E-pH-solvent acceptor number diagram onto the E-pH plane for H = high acceptor number, L = low acceptor number

quantity, and often unknown liquid junction potentials are included in the measurement.

Potential-pH Diagram for 2,4,6-Tri-t-butylphenol.—By blocking the reactive *ortho-* and *para-*positions of a phenol with bulky substituents lacking α-hydrogens, the stability of the aryloxyl radical is greatly enhanced, and the two electron oxidation of the substituted phenol may be observed by electrochemical methods.[5,22] The potential-pH diagram for a compound whose aryloxyl radical (ArO·) and aryloxenium ion (ArO$^+$) are stable is very much more complex than the diagram shown for phenol in Figure 2. Three sets of lines must now be included corresponding to equilibria in the systems ArO·-ArOH/ArO$^-$, ArO$^+$-ArO·, and ArO$^+$-ArOH/ArO$^-$.
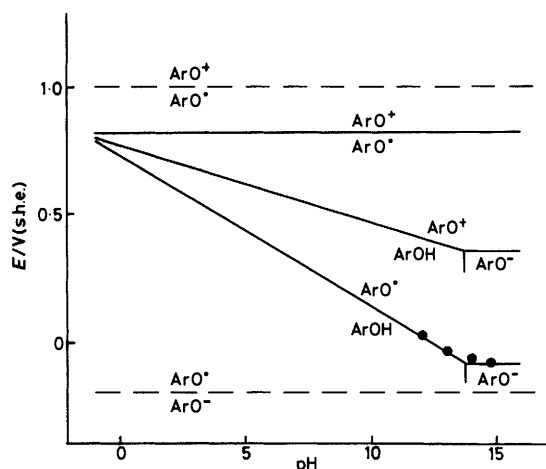
Figure 5. E–pH diagram for 2,4,6-tri-t-butylphenol in 57% aqueous ethanol (bold lines) showing $ArO^{\cdot}$–ArO^- and ArO^+–$ArO^{\cdot}$ equilibria in acetonitrile (dashed lines). Potentials are given as measured against a saturated calomel electrode uncorrected for liquid junction effects

The system we have chosen to describe here, and the one which has been investigated in most detail [14,22] is 2,4,6-tri-t-butylphenol. The potential pH diagram shown in Figure 5 has been constructed from data in the paper by Richards *et al.*[22] who used an aqueous solvent mixture containing 57% by weight of ethanol and a saturated calomel reference electrode.

The potential for reaction (3) at pH 10 was estimated from

$$ArOH \longrightarrow ArO^{\cdot} + H^+ + e \qquad (3)$$

the cyclic voltammograms to be 0.13 V, and used to locate a line of slope $- 0.0592$ V per pH unit. The potential for reaction (4) was given as -0.093 V which fixes the lower horizontal
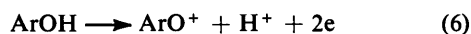
$$ArO^- \longrightarrow ArO^{\cdot} + e \qquad (4)$$
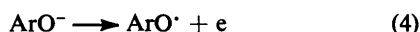
line. The upper horizontal line, corresponding to reaction (5), was estimated as 0.81 V since the anodic peak potential

$$ArO^{\cdot} \longrightarrow ArO^+ + e \qquad (5)$$
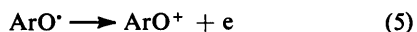
for this reaction was *ca.* 0.84 V (independent of pH) and, for a reversible reaction, the equilibrium potential would be *ca.* 0.03 V lower. The figure of 0.81 V is presumably if anything an overestimate since the reaction is not reversible in the ethanol–water solvent, although it was shown to be reversible in acetonitrile by fast sweep cyclic voltammetry.[22] The diagram so far constructed is essentially similar to that proposed by Waters.[2]

The line for the two-electron oxidation (6) was simply determined from relation (7). It should be noted that below

$$ArOH \longrightarrow ArO^+ + H^+ + 2e \qquad (6)$$

$$E(ArO^+\text{–}ArOH) =$$
$$\tfrac{1}{2}[E(ArO^+\text{–}ArO^{\cdot}) + E(ArO^{\cdot}\text{–}ArOH)] \qquad (7)$$

$pH = pK_a$, this reaction has a potential dependence of -0.0296 V per pH unit, and is not independent of pH as sometimes claimed.[19] The horizontal line for the two-electron reaction (8) was fixed in a similar fashion.

$$ArO^- \longrightarrow ArO^+ + 2e \qquad (8)$$
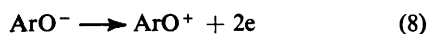
Further points from the E–pH data of Richards *et al.*[22] have been plotted in Figure 5 for comparison. These were originally quoted as quarter-peak potentials, but have been adjusted by the addition of 0.06 V which would give the half-wave potential for a reversible reaction. The apparent pK_a of *ca.* 13.7 determined from Figure 5 for ArOH is in reasonable agreement with the value 13.0 estimated for ArOH in water using the Hammett equations,[23] and allowing for the lower concentration of water in the mixed solvent.

Thus for 2,4,6-tri-t-butylphenol in aqueous ethanol the conditions described by Waters [2] as necessary for disproportionation of the radical to the anion and cation are almost, but not quite, reached. In other solvents, *e.g.* water or with other phenols, disproportionation may occur, but solubility considerations must greatly influence the choice of solvent.
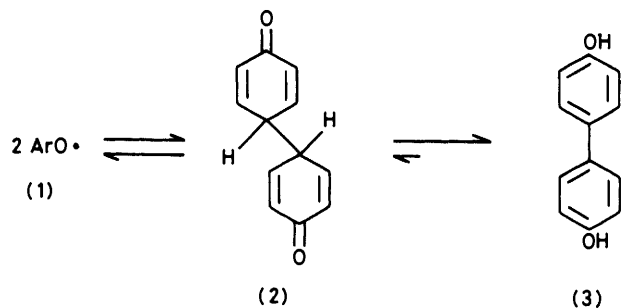
Also shown in the Pourbaix diagram of Figure 5 are the two lines for $ArO^{\cdot}$–ArO^- and ArO^+–$ArO^{\cdot}$ in acetonitrile, which have been located by the estimates of $E^{\ominus}$ for these reactions.[22] This information, although incomplete, indicates that by suitable choice of solvent the potentials in Figure 5 may be lowered or raised in order to make the oxidation more or less selective.

Application to the Chemical Oxidation of Phenols.—The information obtained from Pourbaix diagrams may only be used to predict thermodynamic rather than kinetic results. The lines on an E–pH diagram refer to equal concentrations of the oxidized form and the reduced form. However, during the course of, say, a chemical oxidation, the concentrations of oxidized and reduced forms of both the oxidant and the organic species being oxidized will, in general, be unequal, and will also change during the course of the reaction. Consequently, the potential for each half reaction, as calculated from the Nernst equation, will differ somewhat from the corresponding $E^{\ominus}$.
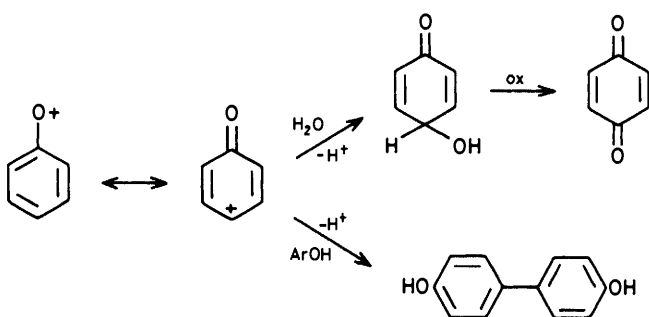
As mentioned earlier, dimerization of aryloxyl radical (1) by either C–C or C–O coupling leads initially to a cyclohexadienone, *e.g.* (2). This reaction is reversible but subsequent tautomeric hydrogen shifts (Scheme 1) then result in a more stable aromatic dimer (3), which may be further oxidized. It has been shown by Mahoney and Weiner [24] that the rate-determining step is the breaking of the C–H bonds in (2), and that this becomes so fast in the presence of added acid that the dimerization is diffusion controlled. Thus the overall reaction is unlikely to be reversible unless the keto-tautomer (2) is of comparable stability to the bisphenol (3), which is unlikely. Removal of two electrons from a phenoxide anion should, in aqueous solution, produce a quinone unless the un-ionized phenol is a much better nucleophile than water, when a dimer should result by electrophilic substitution (Scheme 2). As the pH is decreased the quinone : dimer ratio should therefore increase.

These arguments have already been presented by Waters,[2] but as it now appears that conditions under which aryloxyl radicals disproportionate to cation and anion are seldom likely to be reached in practice, the involvement of aryl-oxenium ions in coupling reactions is only likely to become important when very strong oxidants are used, or when these ions are produced by methods other than oxidation.[4] Their involvement should therefore be reconsidered.
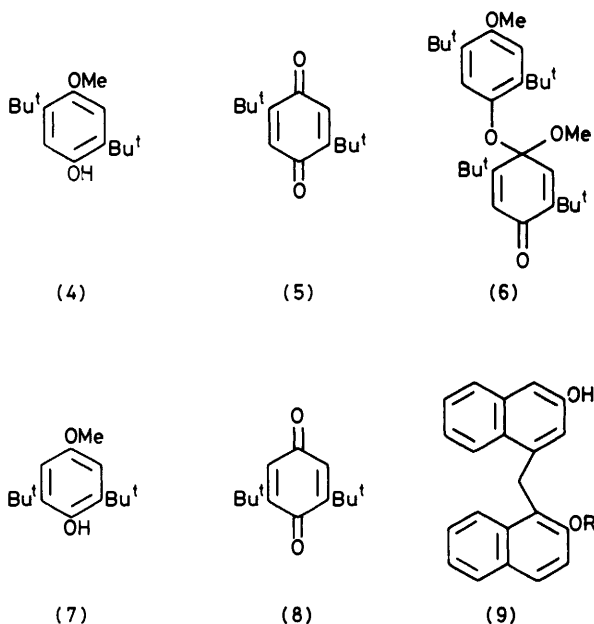
Considering some representative oxidants which are used in aqueous solution, alkaline ferricyanide with an oxidation potential of 0.46 V would appear to be capable only of producing aryloxyl radicals. Of the many reports [25] of the oxidation of monohydric phenols with this reagent, where diamagnetic products have been identified, they all, with one exception, result from oxidative coupling, which thus appears to involve aryloxyl radical intermediates, many of which have

Scheme 1.

Scheme 2.

(4)   (5)   (6)

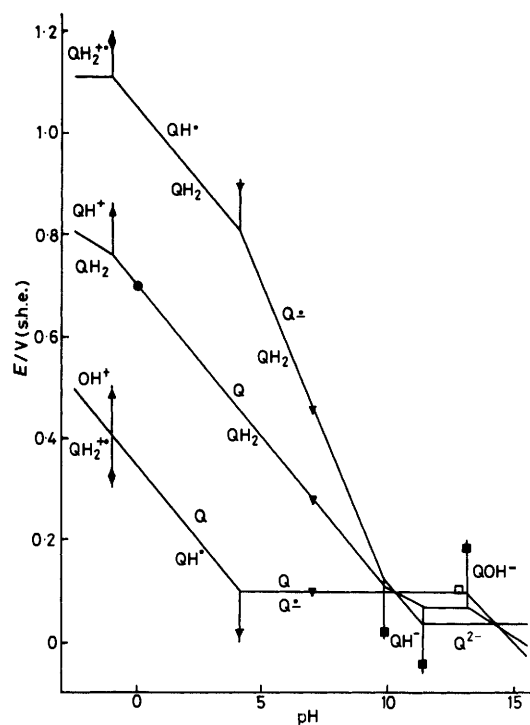(7)   (8)   (9)

Figure 6. The E–pH diagram for benzoquinone–hydroquinone. The sources of data are indicated by the symbol; a solid symbol represents primary data, an open symbol comparison data: ●, refs. 40 and 41; ▲, ref. 42; ■, ref. 36; ▼, ref. 44; ♦, ref. 2

been identified by e.s.r. spectroscopy.[26] This exception is the reported formation of the quinone (5) by ferricyanide oxidation of the phenol (4) in benzene.[27] On repeating this experiment we find that the sole product is the previously described C–O coupled dimer (6), which is converted into a mixture of the quinone (5) and phenol (4) on chromatography or by acid.[28] On the other hand, ferricyanic acid has been shown to oxidize a methanol solution of phenol (7) to the quinone (8) in high yield.[29]

Iron(III) chloride, with an even higher oxidation potential (0.77 V), might thus be expected to be capable of oxidizing phenols with strongly electron-donating groups to aryloxenium ions and thence to quinones. Indeed quite a number of

p-methoxyphenols yield benzoquinones with this reagent,[30] but the mechanistic details are somewhat clouded by the possibility that hydrochloric acid may in fact be hydrolysing an intermediate dienone of type (6).

The much stronger oxidant cerium(IV) invariably oxidizes o- or p-alkoxyphenols to benzoquinones, and like iron(III) chloride effects coupling of phenols which are unsubstituted at the o- or p-positions. Anderson et al.,[31] finding that the same products were produced in the same ratio when p-cresol was oxidized under the same conditions with either cerium(IV) ammonium nitrate or potassium ferricyanide, have concluded that in each case coupling is via the aryloxyl radical. Cerium(IV) thus appears able to produce aryloxenium ions from phenols of low potential, but coupling, when favourable, is still more rapid with the radical than further oxidation to the cation.

It is also worth noting Hewitt's observation that with even the strongest oxidants the ether (9) gave a coupled dimer rather than intramolecular electrophilic substitution.[32] This result, however, may reflect a greater delocalization of the positive charge of a phenoxenium ion onto carbon, as predicted by Waters.[2]

In the oxidation of bisphenols to intramolecularly coupled products, attempts to observe simultaneously radicals derived from both rings of the same molecule have so far been unsuccessful, but it is likely that once a second electron is removed coupling will take place before an e.s.r. spectrum can be recorded.[33,34] The alternative two-electron oxidation of one phenolic oxygen to a phenoxenium ion, followed by intramolecular electrophilic substitution, seems most unlikely in comparison with removal of one electron from each phenolic oxygen.

The E–pH Diagram for the Quinone–Semiquinone–Hydroquinone System in Water.—We will now consider the oxid-

ation of 1,4-dihydroxybenzene. In contrast to the oxidation of a phenol, the oxidation products of this compound are very much more stable, and so it is possible to obtain reliable values for the relevant equilibrium potentials. In constructing the E–pH diagram shown in Figure 6, a number of complications, inherent in the system have been neglected for simplicity. The most important of these is the fact that quinone undergoes irreversible decomposition in strongly alkaline solution.[35,36] In addition, no account has been taken of the possibility of further protonations of both the oxidized and reduced species which can occur in very strong acid [37,38] and, particularly, superacid media.[39] The formation of quinhydrone has also been neglected.

In Figure 6 (see caption), a distinction has been made between those data points used to determine the form of the diagram, and those data points which have been obtained from other sources and are included for comparison.

(a) *Quinone–hydroquinone*. The first set of equilibria to be considered are those between quinone (Q) and hydroquinone (QH₂). Equilibrium (9) is represented on the Pourbaix

$$Q + 2H^+ + 2e \rightleftharpoons QH_2 \qquad (9)$$

diagram by a line of slope -0.0592 V per pH unit passing through $E^{\ominus} = 0.6998$ V.[40,41] In a sufficiently strong acid solution, the quinone is protonated to give QH^+. Equilibrium (10) is represented by a vertical line at $pH = pK_a = -1.0$.[42] Equilibrium (11) which corresponds to a line on the E–pH
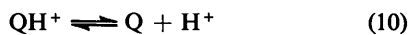
$$QH^+ \rightleftharpoons Q + H^+ \qquad (10)$$

$$QH^+ + H^+ + 2e \rightleftharpoons QH_2 \qquad (11)$$

diagram of slope -0.0296 V per pH unit, is thus dominant above a pH of -1.0.

As the basicity of the solution is increased, the hydroquinone undergoes two successive deprotonations with pK_a (QH₂) = 9.85 [36,43] and pK_a (QH⁻) = 11.4.[36,43] These are again represented by vertical lines. When $9.85 < pH < 11.4$, the equilibrium is (12) giving a line of slope -0.0296 V per pH unit. For $pH > 11.4$, equilibrium (13) gives a line of zero

$$Q + H^+ + 2e \longrightarrow QH^- \qquad (12)$$

$$Q + 2e \rightleftharpoons Q^{2-} \qquad (13)$$
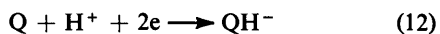
slope. At a sufficiently high pH, Q forms a reversible adduct with OH⁻ [reaction (14)], the equilibrium constant [36] being 8.3 mol⁻¹ dm³. This can, however, be simply considered another

(Q)   (QOH⁻)
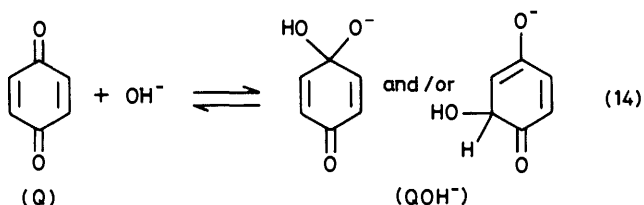
acid–base equilibrium with pK_a 13.1. Above pH 13.1 the redox equilibrium is then (15) which is represented by a line of slope -0.0296 V per pH unit.

$$QOH^- + 2e \rightleftharpoons Q^{2-} + OH^- \qquad (15)$$
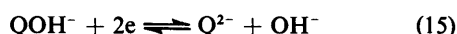
(b) *Quinone–semiquinone*. A set of equilibria will also exist between quinone and semiquinone (QH·). It is convenient to first locate the line for equilibrium (16). This reaction has an

equilibrium potential of 0.009 V at pH 7,[44] and is independent of pH above pH = pK_a (QH·) = 4.1.[44] The position of this
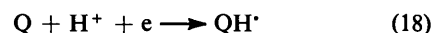
$$Q + e \rightleftharpoons Q^{-\cdot} \qquad (16)$$

line can also be calculated relative to the Q–Q²⁻ line from the equilibrium constant for the disproportion reaction (17).

$$2Q^{-\cdot} \rightleftharpoons Q + Q^{2-} \qquad (17)$$
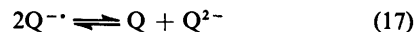
Using the data of Bishop and Tong [36] and Diebler *et al.*,[45] this locates the line as being 0.040 V positive of the Q–Q²⁻ line.

Below a pH of 4.1, the equilibrium reaction is (18) which

$$Q + H^+ + e \longrightarrow QH^{\cdot} \qquad (18)$$

gives a line of slope -0.0592 V per pH unit. Above pH *ca.* -1,[2] QH· is protonated to QH₂⁺· and Q is protonated to QH⁺ and so the redox reaction becomes (19) which is also a

$$QH^+ + H^+ + e \rightleftharpoons QH_2^{+\cdot} \qquad (19)$$

line of slope -0.592 V per pH unit. The situation where both the oxidized and reduced species have an identical acid dissociation constant is very unusual, but it should be noted that these pK_a values are approximate, and may be considerably in error.[46] This is of little concern as a solution with $pH < -1$ is not normally of interest.

Above pH 13.1, the adduct QOH⁻ is the stable oxidized species with reaction (20) giving a slope of -0.592 V per pH unit.

$$QOH^- + e \rightleftharpoons Q^{+\cdot} + OH^- \qquad (20)$$
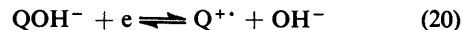
(c) *Semiquinone–hydroquinone*. The E–pH diagram for the semiquinone–hydroquinone system was constructed in a similar fashion to that described in the two previous sections. The line of slope 0.118 V per pH unit for reaction (21) was

$$Q^{-\cdot} + 2H^+ + e \rightleftharpoons QH_2 \qquad (21)$$

located by a value for the equilibrium potential at pH 7 of 0.459 V.[44] All other lines follow from the acidity constants already given. The diagram could also have been calculated from the diagrams for Q–QH₂ and Q–QH·.

The Effect of Adding Organic Solvents.—As with phenol, it should be possible, at least in principle, to construct a three dimensional Pourbaix diagram for the quinone–semiquinone–hydroquinone system in which the third dimension is some parameter, such as the acceptor number, characteristic of the solvent system.

It is known that in organic or mixed aqueous–organic solvents, the semiquinone radical and radical ion are stabilized relative to the hydroquinone species.[42] The potential difference between the lines Q–Q⁻· and Q–Q²⁻ is therefore increased, and the pH above which Q⁻· is the most stable species is lowered. As a consequence, it is much easier to observe the two-step electrochemical reduction of quinones in aprotic media than in water.[42] Moreover, the difference in potential between the Q–Q⁻· and Q⁻·–Q²⁻ couples has been shown to increase linearly with the pK_a for solvent self-ionization.[47] In addition, the potential of the Q–Q⁻· couple has been found to shift to more negative values as the acceptor number of the solvent is decreased.[21] There is, however, insufficient information available at the present time for a diagram to be constructed accurately.

Application of the E–pH *Diagram for the Quinone–Semiquinone–Hydroquinone System.*—(a) *Chemical studies.* As
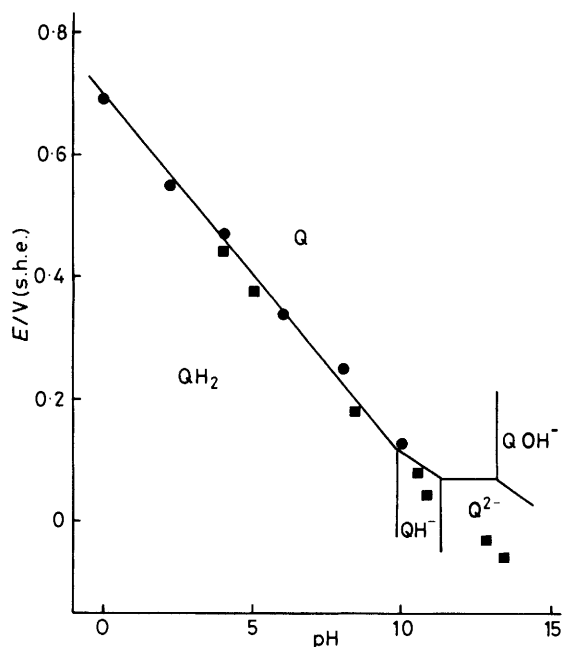
651

Figure 7. A portion of the E–pH diagram for benzoquinone showing the Q–QH$_2$ equilibria and associated acid–base equilibria. Superimposed point data are from ●, ref. 7 and ■, ref. 48

which specific reactions could be effected, and better understanding of the processes involved.

already noted, a Pourbaix diagram such as Figure 6 defines the conditions of potential and pH under which any species in the system will be stable. For example, it can be seen from Figure 6 that the semiquinone radical anion is the most stable species in the chisel-shaped region starting at pH 10.2 and lying within the potentials 0.04 and 0.10 V. High concentrations of Q$^{-•}$ have indeed been observed in this region in flow or pulse experiments,[36,45] but the Q$^{-•}$ lifetime is short due to the instability of the system with respect to hydroxide.

It follows from Figure 6 that below a pH of *ca.* 10, the reduction of Q or the oxidation of QH$_2$ is likely to proceed by a two-electron step. If the semiquinone is formed, it can only exist in low concentrations when the system is at equilibrium, or it can exist as a metastable species which will disproportionate. Above pH 10, the reduction of Q and the oxidation of Q^{2-} is likely to proceed by two one-electron steps.

(b) *Electrochemical studies.* In this section, we will show how the Pourbaix diagram (Figure 6) can be used to interpret the results of some electrochemical studies on carbon and mercury electrodes.

$E_{\frac{1}{2}}$ *versus* pH data for the reduction of Q on carbon[7] and mercury[48] are shown superimposed on a portion of the Pourbaix diagram in Figure 7.

The points lie scattered about the Q–QH$_2$ line, and so it would seem that two electrons are transferred according to reaction (22). However, it is curious that the data points of

$$Q + 2H^+ + 2e \longrightarrow QH_2 \qquad (22)$$
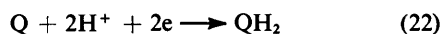
Flaig *et al.*[48] for the reduction of quinone on mercury continue to follow the equilibrium line down past pH 10. At high pH values, the formation of the protonated hydroquinone which is unstable seems unlikely.

Conclusions.—In conclusion we would like to point out the possibility of applying this sort of treatment to other classes of organic compounds for which oxidation-reduction reactions involving proton transfer can occur. Hopefully, this should allow more accurate prediction of conditions under

References

1 M. Pourbaix, 'Atlas of Electrochemical Equilibria in Aqueous Solutions,' Pergamon Press, Oxford, 1966.
2 W. A. Waters, *J. Chem. Soc. B*, 1971, 2026.
3 F. R. Hewgill, in ' Free Radical Reactions,' ed. W. A. Waters, Butterworths, London, 1973, ch. 10, p. 168.
4 R. A. Abramovitch, G. Alvernhe, R. Bartnik, N. L. Dassanayake, M. N. Inbasekaran, and S. Kato, *J. Am. Chem. Soc.*, 1981, **103**, 4558.
5 K. Dimroth and K. J. Kraft, *Chem. Ber.*, 1966, **99**, 264.
6 P. Delahay, ' New Instrumental Methods in Electrochemistry,' Interscience, New York, 1954.
7 R. N. Adams, ' Electrochemistry at Solid Electrodes,' Dekker, New York, 1969.
8 L. Papouchado, R. W. Sandford, G. Petrie, and R. N. Adams, *J. Electroanal. Chem.*, 1975, **65**, 275.
9 G. Kortüm, W. Vogel, and K. Andrussow, ' Dissociation Constants of Organic Acids in Aqueous Solution,' Butterworth, London, 1961.
10 J. F. Hedenberg and H. Frieser, *Anal. Chem.*, 1953, **25**, 1355.
11 F. P. Bub, K. Wisser, W. J. Lorenz, and W. Heimann, *Ber. Bunsenges. Phys. Chem.*, 1973, **77**, 823.
12 Yu. V. Vodzinskii, A. A. Vasil'eva, and I. A. Korshunov, *Zh. Obshch. Khim.*, 1969, **39**, 1196.
13 G. E. Penketh, *J. appl. Chem.*, 1957, **7**, 512.
14 A. B. Suttie, *Tetrahedron Lett.*, 1969, **12**, 953.
15 R. Cecil and J. S. Littler, *J. Chem. Soc. B*, 1968, 1420.
16 G. Popp and N. C. Reitz, *J. Org. Chem.*, 1972, **37**, 3646.
17 C. H. Rochester in, ' The Chemistry of the Hydroxyl Group,' ed. S. Patai, Interscience, London, 1971, part 1, ch. 7, p. 373.
18 S. D. Ross, M. Finkelstein, and E. J. Rudd, 'Anodic Oxidations,' Academic Press, New York, 1975, p. 273.
19 F. J. Vermillion, jun., and I. A. Pearl, *J. Electrochem. Soc.*, 1964, **111**, 1392.
20 J. S. Hine, ' Physical Organic Chemistry,' McGraw-Hill, New York, 1962, ch. 2.
21 J. S. Jaworski, E. Lesniewska, and M. Kalinowski, *J. Electroanal. Chem.*, 1979, **105**, 329.
22 J. A. Richards, P. E. Whitson, and D. H. Evans, *J. Electroanal. Chem.*, 1965, **63**, 311.
23 G. B. Barlin and D. D. Perrin, *Quart. Rev.*, 1966, **20**, 75.
24 L. R. Mahoney and S. A. Weiner, *J. Am. Chem. Soc.*, 1972, **94**, 585, 1412.
25 M. L. Mihailovic and Z. Cekovic, ref. 17, ch. 10.
26 H. B. Stegmann in Landolt-Börnstein, New Series, Springer-Verlag, Berlin, 1979, Part 21, vol. 9, ch. 8.
27 E. Müller, H. Kaufmann, and A. Rieker, *Liebig's Ann. Chem.*, 1964, **671**, 61.
28 C. J. R. Adderley and F. R. Hewgill, *J. Chem. Soc. C*, 1968, 1434.
29 L. Taimr and J. Pospisil, *Tetrahedron Lett.*, 1971, 2809.
30 H. Ulrich and R. Richter in Houben-Weyl, ' Methoden der Organischen Chemie,' Georg Thieme Verlag, Stuttgart, 1977, vol. VII/3a.
31 R. A. Anderson, D. T. Dalgleish, D. C. Nonhebel, and P. L. Pauson, *J. Chem. Res. (S)*, 1977, 12.
32 D. G. Hewitt, *J. Chem. Soc. C*, 1971, 1750.
33 S. M. Colegate, F. R. Hewgill, and G. B. Howie, *Aust. J. Chem.*, 1975, **28**, 343.
34 F. R. Hewgill and M. C. Pass, *Tetrahedron Lett.*, 1981, **22**, 2125.
35 K. T. Finlay in ' The Chemistry of the Quinonoid Compounds,' ed. S. Patai, Wiley, New York, 1974, Part 2, ch. 17, p. 942.
36 C. A. Bishop and L. K. J. Tong, *J. Am. Chem. Soc.*, 1965, **87**, 501.
37 G. A. Olah and M. Calin, *J. Am. Chem. Soc.*, 1968, **90**, 4672.
38 R. C. Paul, V. P. Kapila, J. K. Puri, and K. C. Malhotra, *Indian J. Chem.*, 1971, **9**, 992.

39 A. B. Hadid, P. Rimmelin, J. Sommer, and J. Devynck, *J. Chem. Soc., Perkin Trans. 2*, 1982, 269.

40 R. C. Weast, ' C.R.C. Handbook of Chemistry and Physics,' C.R.C. Press, Cleveland, 1980, 60th edn.

41 D. J. G. Ives and G. J. Jantz, ' Reference Electrodes, Theory and Practice,' Academic Press, New York, 1961.

42 J. Q. Chambers, ref. 35.

43 J. H. Baxendale and H. R. Hardy, *Trans. Faraday Soc.*, 1953, **49**, 1140.

44 Y. A. Ilan, G. Czapski, and D. Meisel, *Biochim. Biophys. Acta*, 1976, **430**, 209.

45 H. Diebler, M. Eigen, and P. Mathies, *Z. Naturforsch.*, 1961, **16**, 629.

46 A. Beauchamp and R. C. Benoit, *Can. J. Chem.*, 1966, **44**, 1607.

47 L. Ya Kheifets, Yu. P. Ponomarev, and N. A. Sobina, *Zh. Obshch. Khim.*, 1973, **43**, 705.

48 W. Flaig, H. Beutelspacher, H. Riemer, and E. Kälke, *Liebig's Ann. Chem.*, 1968, **719**, 96.